AD_____

Award Number:

W81XWH-09-1-0603

TITLE:

Highly Selective Tumor Targeting with Phage Display and Laser Capture Microdissection

PRINCIPAL INVESTIGATOR:

David Krag, MD

CONTRACTING ORGANIZATION:

University of Vermont and State Agricultural College
Burlington, VT 05405

REPORT DATE:

September 2010

TYPE OF REPORT:

Final

PREPARED FOR: **U.S. Army Medical Research and Materiel Command**
Fort Detrick, Maryland 21702-5012

DISTRIBUTION STATEMENT:

☒ Approved for public release; distribution unlimited

REPORT DOCUMENTATION PAGE

Form Approved
OMB No. 0704-0188

1. REPORT DATE *(DD-MM-YYYY)*	2. REPORT TYPE	3. DATES COVERED *(From - To)*
01-09-2010	Final Report	15 Aug 2009 - 14 Aug 2010

4. TITLE AND SUBTITLE
Highly Selective Tumor Targeting with Phage Display and Laser Capture Microdissection

5a. CONTRACT NUMBER

5b. GRANT NUMBER
W81XWH-09-1-0603

5c. PROGRAM ELEMENT NUMBER

6. AUTHOR(S)
David Krag, MD
Yu-jing Sun

Email: David.Krag@uvm.edu

5d. PROJECT NUMBER

5e. TASK NUMBER

5f. WORK UNIT NUMBER

7. PERFORMING ORGANIZATION NAME(S) AND ADDRESS(ES)
University of Vermont and State Agricultural College
Burlington, VT 05405

8. PERFORMING ORGANIZATION REPORT NUMBER

9. SPONSORING / MONITORING AGENCY NAME(S) AND ADDRESS(ES)
U.S. Army Medical Research
And Materiel Command
Fort Detrick, MD 21702-5012

10. SPONSOR/MONITOR'S ACRONYM(S)

11. SPONSOR/MONITOR'S REPORT NUMBER(S)

12. DISTRIBUTION / AVAILABILITY STATEMENT

Approved for public release; distribution unlimited

13. SUPPLEMENTARY NOTES

14. ABSTRACT
BT474 xenograft modal was successfully established in our lab. Tumor stroma enriched BT474 modal was tested using BT474 cell lines and human breast fibroblast cell lines. Mixture of BT474 cells and human breast fibroblast cells did not yield a xenograft with sufficient fibroblast component. LCM panning of human tumor specimens was performed with selection on blood vessels. More than 200 monoclones were evaluated for binding. Although clones were identified with some blood vessel binding the affinity was too low for subsequent in vivo imaging studies. Three BT474 cell binding scFv clones 799, 785, 794 were selected and single chain antibody of these clones were successfully expressed, purified and prepared in large scale. These scFvs were evaluated in vivo but preferential binding to the tumor relative to normal tissue (especially kidney) was not sufficient. Antibodies that bind different targets on BT474 cells were selected and successfully labeled infrared fluorescence dyes of different wavelengths. The labeling procedure was shown to not interfere with antibody affinity. The labeled antibodies (Herceptin and anti-EpCAM) were administered in vivo and successfully demonstrated to bind preferentially and additively in the tumor xenograft.

15. SUBJECT TERMS
Phage display, panning, Laser capture microdissection(LCM), in vivo imaging, breast cancer, xenograft

16. SECURITY CLASSIFICATION OF:			17. LIMITATION OF ABSTRACT	18. NUMBER OF PAGES	19a. NAME OF RESPONSIBLE PERSON
a. REPORT	b. ABSTRACT	c. THIS PAGE			USAMRMC
U	U	U	UU	19	19b. TELEPHONE NUMBER *(include area code)*

Table of Contents

Page

Introduction

We report here the summary of the research work done over this past year. The goal was to increase the uptake of anticancer antibodies in a breast cancer. The strategy was to target different elements of the solid breast cancer with antibodies and demonstrate increased in vivo tumor accumulation of these antibodies.

Body

Task 1. Identify three sets of phage-displayed antibodies that bind selectively to breast cancer cells, tumor blood vessels, and tumor stroma cells from a solid breast cancer xenograft tissue. (months 1-6)

1. Establish breast cancer xenografts (months 1-2)

1a. Prepare breast cancer xenograft model

A xenograft breast cancer model is necessary to assess in vivo uptake of the tumor-targeting antibodies. Our goal was to have multiple tumor elements present; this included tumor cells and noncancer tumor support cells (fibroblastic stromal cells and blood vessels). Implantation of BT474 breast cancer cells reliably led to solid tumor growth but did not yield a fibroblast stromal response from the mouse. However, implantation of only BT474 breast cancer cells grew almost exclusively as dense cancer cells without significant supporting stroma. Figure 1 shows a representative histological structure of BT474 xenograft generated from BT474 tumor cell lines.

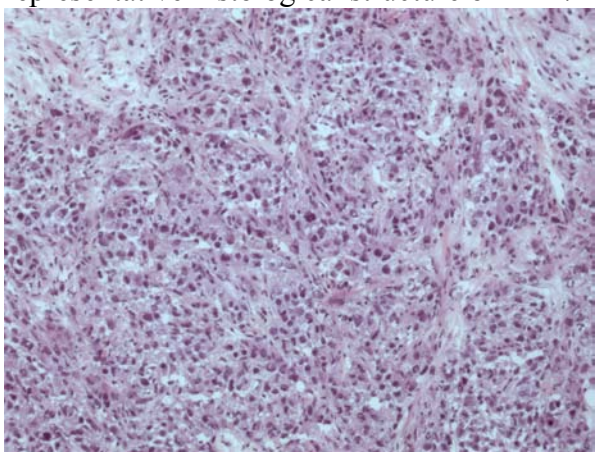

Figure 1: BT474 xenograft tissue showing almost pure malignant cell composition with minimal amount of mixed stroma.

Co-implantation of breast cancer cells simultaneously with breast fibroblasts were reported to show scirrhous or trabecular growth pattern with extensive fibrosis. *(Yashiro, Ikeda et al. 2005)* We therefore implanted two different human cell types simultaneously into the mouse host. This included BT474 breast cancer cells and human breast fibroblast cells which were cultured from discarded surgical breast reduction specimens. Multiple low passage breast fibroblast cell lines were evaluated. After 2 passages, fibroblast cell character was tested by morphology and confirmed by staining with Vimentin and cytokeratin. Only one of these yielded sufficient growth with a doubling time of 2.5 days.

Eight 5-week-old nude mice were divided into 2 groups. One group of 5 mice had subcutaneous implantation of $5x10^6$ BT474 cells and 5 $x10^6$ human breast fibroblast cells. The control group of 3 mice had subcutaneous implantation of 5 $x10^6$ BT474 cells only. Tumor size was measured by caliper 3 times a week until tumors reached the target size at 1000mm3. Figure 2 shows the growing pattern of these two groups.

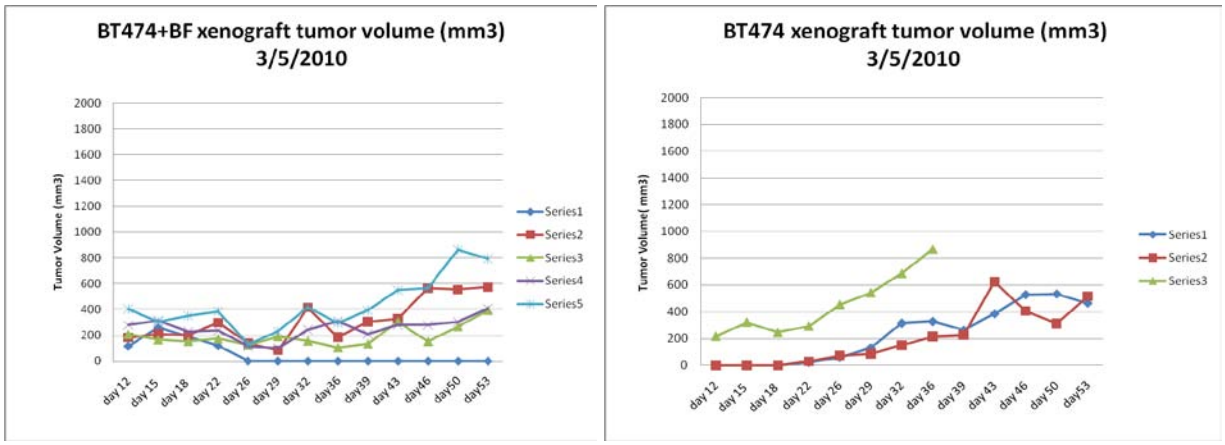

Figure 2: Growing pattern of BT474 plus breast fibroblasts (BF) and BT474 only in nude mice.

After 8 weeks, the mice were sacrificed and tumor tissue harvested for histological analysis. Figure 3 shows the histological structure of H&E stained tumor tissues. No clear histological difference was found between the tumors generated from BT474 cells alone versus BT474 cells mixed with human breast fibroblasts. These results show that co-culture of human normal breast fibroblast cells did not provide a solid tumor model with multiple cell types. Further compounding the problem of multiple cell xenograft was that adding human breast fibroblasts to BT474 cells caused the xenografts to grow more slowly and in one of five mice the tumor did not grow at all.

Decreased growth and lack of suitable fibroblast tissue in the xenograft was not consistent with our expectations based on published literature. These phenomena may indicate that the mismatching of cell surface MHC molecular caused some problems to one or both cells as BT474 cells and human normal breast fibroblast cells are derived from different individuals. Using normal and tumor cells derived from one patient may solve the problem, but this approach was not within the scope of this grant.

These results may have provided sufficient mixed cells for labeling with antibodies but not enough tissue for panning purposes. In order to derive antibody binding to different cellular elements, an alternative strategy was employed (see section 1b, below).

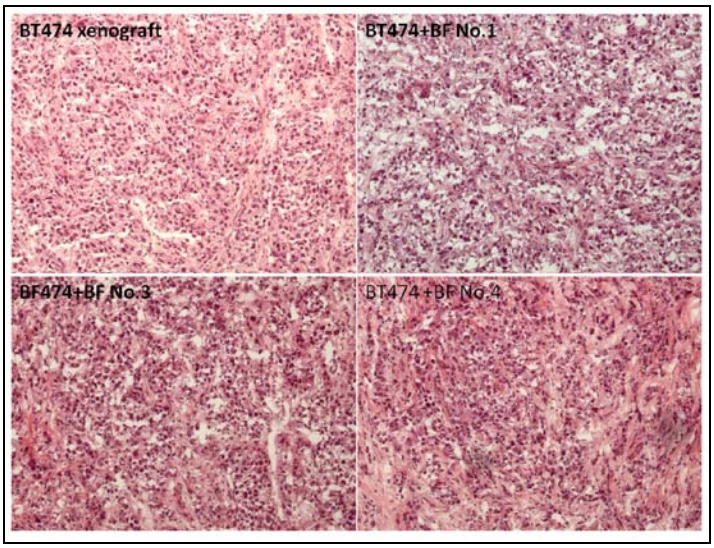

Figure 3: BT474 xenograft and BT474+ breast fibroblasts (BF) xenograft. Each tissue shows the same dense cancer cell solid structure with very limited portion of mixed stroma.

1b. Panning on tumor blood vessels with laser capture microdissection (LCM). (months 3-4)

As the BT474 tumor xenograft established in 1a (above) did not provide ample stroma as a target for panning, we panned on selected archived human breast cancer frozen sections derived from discarded surgical material.

Human cancer specimens were chosen with sufficient nonmalignant elements for panning. $1x10^{12}$TU phage library in 200 ul binding buffer (1× PBS with 0.05% Tween-20, 10% goat serum, and 0.2% casein blocker) were put directly on the tissue section for 2 hours in a moist box at room temperature. After incubation, slides were rinsed 6 times in PBST and blood vessels were labeled with anti-human CD146 antibodies. Unbound phages clones were rinsed off and binding phage to tumor blood vessel collected under fluorescent LCM. A total of 200 blood vessel pieces are collected for binding clones' recovery after phage panning. Figure 4 shows the blood vessel LCM capture steps. The phage clones attached to blood vessel were recovered by host bacterial infection and selected on TYE-ampicillin plates. The first panning outputs were pooled and amplified. 1×10^{12} TU of amplified phage were used for the next round of panning. After two rounds of panning, individual colonies were randomly selected from the panning output for binding assay and DNA sequence analyses.

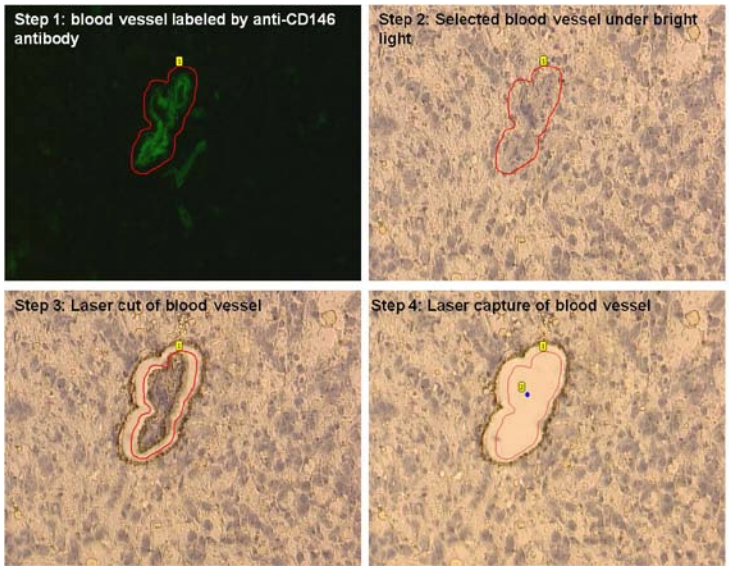

Figure 4: LCM process of blood vessel (BV) in tumor tissue. *Blood vessel is visualized by CD146 IF staining (step 1) and detoured (red line around BV, step 2). Under bright light, BV is cut (step 3) and captured (step 4) by laser beams.*

Table 1: Panning input and output of LCM panning experiment on blood vessel.

	Input (TU)	Output (TU)
1st round	1x10^{12} TU phage libraries (Tomlinson I scFv phage display library)	204
2nd round	1x10^{12} TU amplified 1st panning output	567

Table 1 shows an example of the recovery efficiency of the blood vessel panning experiments. The output phages were only in the hundreds of TUs which is low compared to similar panning experiments against other non-blood vessel targets. This may have been caused by the small size and fragile character of blood vessel.

1c. Identify specific binding antibodies to tumor blood vessels by immunofluorescence (IF) microscopy. (months 5-6)

Individual phage clone recovered from the blood vessel panning experiments were screened on the same tumor frozen sections using phage IF microscopy. 240 randomly selected individual phage monoclones were amplified and normalized by chemititration (Shukla and Krag 2005). 1x10^{12} TU of each clone were incubated with tissue sections in 24-well plates at room temperature with shaking for 2 hours. After incubation, slides were rinsed 10 times in PBST (PBS containing 0.1% tween-20) and once in PBS. Slides were incubated with rabbit anti-phage antibody and mouse anti-human CD146 antibody cocktail. The phage were labeled with Alex 488 conjugated chicken anti-rabbit antibody and blood vessels were visualized with Alex 568 conjugated goat anti-mouse secondary antibody. The slides were observed under fluorescence microscope. Naïve phage library and wild type phage (KM13 helper phage) were used as negative controls.

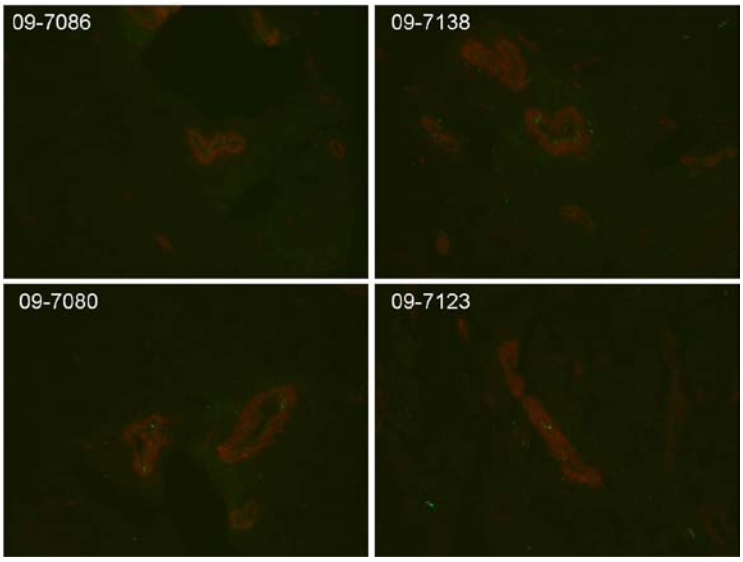

Figure 5: IF staining analysis of phage recovered from blood vessel panning experiments. Phage particles are labeled green; blood vessels are labeled red.

Figure 5 shows examples of 4 different clones binding to red stained blood vessels. After screening 240 clones, only weak blood vessel binding clones were identified. The pattern of staining overall was weak. A few clones showed brighter staining on only about 5% of the blood vessels. These results did not yield a phage-derived antibody that showed sufficient binding to blood vessels to be used in the in vivo imaging experiments.

Task 2. Determination of in vivo binding of scFv antibodies to tumor xenografts. (months 7-12)

Our research goal was to demonstrate increased overall tumor uptake by using antibodies that target different elements of the tumor. The mouse mixed cell tumor model did not yield satisfactory solid tumor with mixed elements for phage panning. Also, panning on human tumors that did have sufficient blood vessels did not yield blood vessel-binding phage with adequate affinity suitable for in vivo imaging. We therefore moved to a modified strategy and attempt to identify BT474-binding phage from a pool of breast cancer cell-binding phage antibodies derived from prior experiments. The prior experiments were performed using disaggregated cancer cells derived from fresh harvested but discarded breast cancer specimens. (2a. below)

2a. Antibody expression, purification, and labeling preparations. (months 7-8)

2a-1. Several positive binding phage scFvs were previously selected from clinic breast cancer tissue in our lab using filter unit panning methods.(Shukla and Krag 2005) Several of these phage clones were evaluated for binding to BT474 cells (Figure 6). Clone binding was done by placing 50,000 BT474 cells in each well of a 96-well plate. Individual phage clones were incubated in each well and then rinsed. Bound phages were labeled with HRP conjugated anti-phage antibody. Naive phage library was used as control.

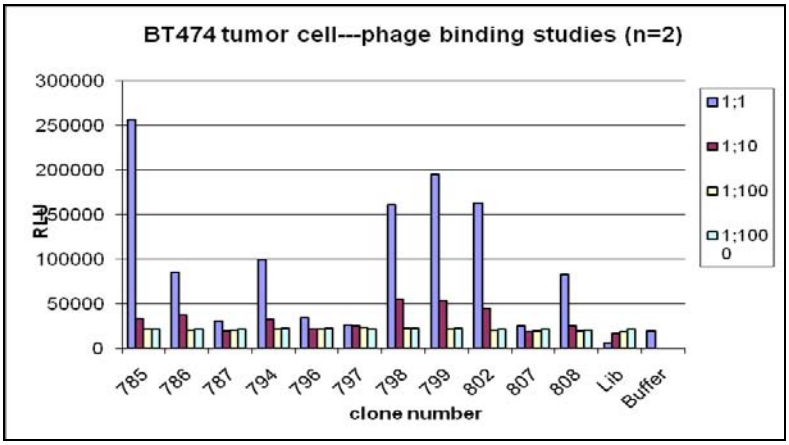

Figure 6: Binding of individual phage clones incubated with BT474 cells in 96-well plates.

2a-2. The three best binding clones, 799, 794, and 785, were then evaluated for binding to normal mouse tissue. This was important to evaluate since background staining of these clones on mouse tissue would interfere with in vivo tumor binding assessment.

Normal mouse tissue frozen sections were prepared for phage IF staining. The normal mouse tissues included heart, liver, spleen, kidney, and skin. $1x10^{13}$ TU/ml of phage clones 799, 794, and 785 were incubated with each tissue section. After rinsing, bound phages were labeled with Alexa 488 conjugated anti-phage antibody. Evaluation of binding was done with IF microscopy. Naïve phage library was used as control. Fig 7 shows the mouse normal tissue binding profile of clones 799, 794, and 785 compared to naïve phage binding to the same tissues. The result shows that clones 799, 794, and 785 didn't bind specifically to mouse normal tissues.

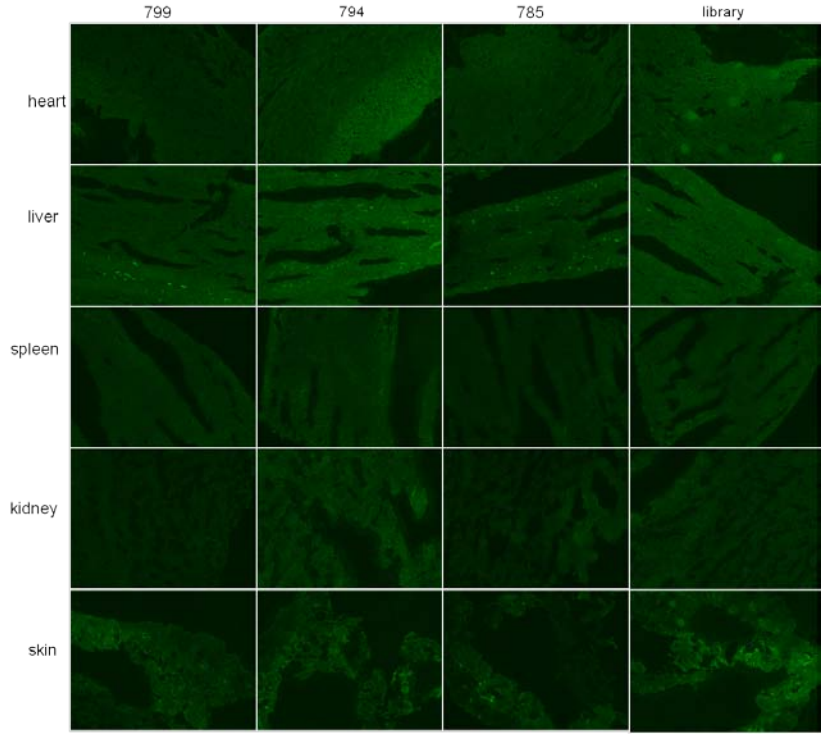

Figure 7: Clones 799, 794, and 785 phage clones binding profile on normal mouse tissue. Phage staining was observed by Alexa 488 conjugated anti-phage antibodies. Naive phage library was used as control.

2a-3. Production and purification of soluble scFv antibody

Preparation for in vivo infusion of scFvs requires generation of sufficient amounts of soluble scFv not attached to phage particles. ScFvs fused to the pIII coat protein of phage were converted to soluble scFv proteins by infection in *E coli* HB2151 as described in the literature. (Golchin and Aitken 2008) *E coli* HB2151 (OD 0.4) was incubated with an aliquot of the selected phage clone at 37°C for one hour, then plated onto TYE agar containing 100µg/ mL ampicillin and 1% (v/v) glucose for overnight growth at 30°C. Individual colonies were picked and saved in 20% glycerol for soluble scFv production. The HB2151 phage overnight culture was diluted 1:100 into 200ml 2×YT containing 100µg/mL ampicillin and 0.1% glucose. The bacterial culture was shaken at 37°C until the culture density reached to 0.9 OD^{600}. Then the expression of the scFvs was induced by addition of 25 ml 2×TY containing 100µg/mL ampicillin and 9 mM IPTG. Incubation continued for 20 hours at 30°C. The bacterial culture was centrifuged at 3000rpm for 15 minutes and the supernatant used for scFv purification.

For purification of scFv in supernatants, centrifuge columns (Pierce) packed with protein-L resin (Pierce) were used. Soluble scFv proteins were eluted with 0.1 M glycine at pH 3.0 and immediately neutralized by 1M Tris buffer pH 9.0. Eluted fractions were analyzed by SDS-PAGE. The fractions found to contain purified scFv were pooled, concentrated 100-fold (Amicon Ultra-4 centrifugal filter, Millipore, UK), and stored at −20°C in PBS with 20% glycerol. SDS-PAGE test showed that scFvs 785 and 794 had good purity and good quantity (see Figure 8).

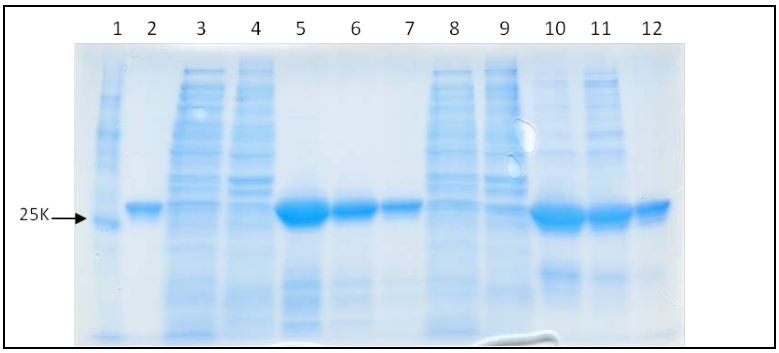

Figure 8: SDS-PAGE gel of purified scFv 799, 794, and 785. Lane 1 is protein marker. Lane 2 is purified scFv 799. Lanes 5, 6, and 7 are purified and concentrated 794 scFv. Lanes 10, 11, and 12 are purified and concentrated 785 scFv.

2a-4. Purified scFv IF stain on BT474 cell and xenograft tissue

It is important to determine that the purified scFv derived from the phage particle still has binding to its target. The binding affinity of purified scFv 799, 785, 794, and negative control 807 were tested using IF staining on BT474 whole cell slides and xenograft tissue sections. Fig 9 shows scFv 799, 794, and 785 had strong binding to BT474 whole cell frozen slides compared with negative clone 807 and negative control of secondary antibody only. Fig 10 shows the IF staining results of these same scFvs antibodies on BT474 tumor xenograft tissue. 9G6 antibody to ErbB2 is used as positive control. Green label shows scFv and 9G6 antibody binding and blue is DAPI nuclear stain.

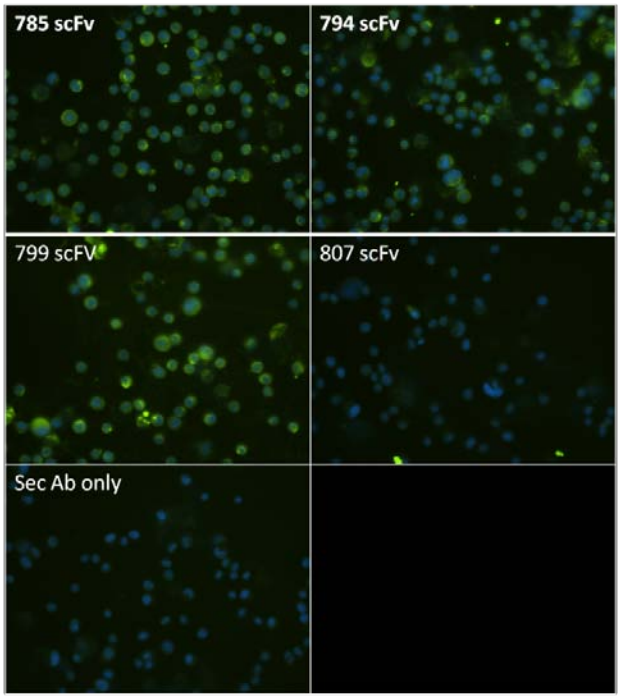

Figure 9: scFv antibodies 799, 794 and 785 IF staining on BT474 whole cell frozen slides. scFv antibody binding was tested by Alexa 488 conjugated anti-His tag antibody. ScFv 807 was a negative binding antibody selected from the same phage library.

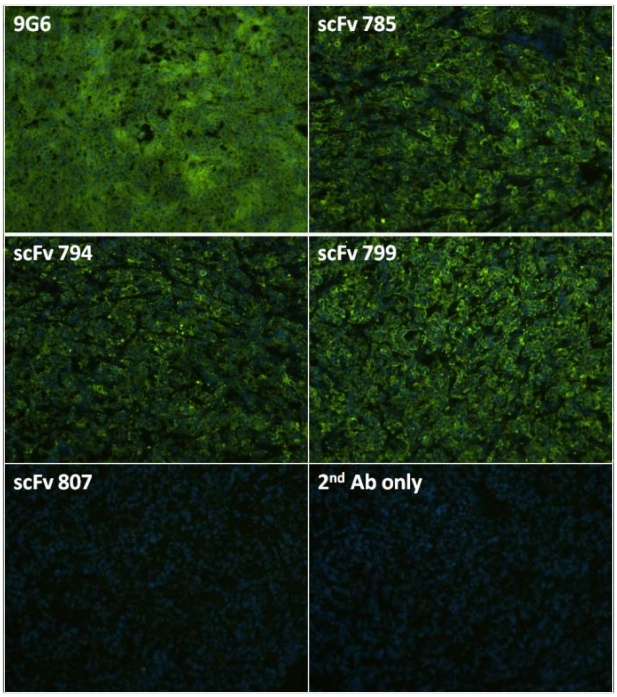

Figure 10: scFv antibody 799, 794 and 785 IF staining on BT474 xenograft tissue frozen sections. scFv antibody binding was tested by Alexa 488 conjugated anti-His tag antibody. ScFv 807 was negative binding antibody selected from the same phage library. 9G6 is an anti-ErBb2 antibody used as positive control.

These results show purified 799, 794, and 785 scFv have specific binding to BT474 whole cells and mouse xenograft tissue with low cross reaction to major mice organ and tissue.

2b. Near infrared (NLR) fluorescence in vivo imaging of mouse whole body, tissue, and organs. (months 9-12)

2b-1. In vivo optical imaging antibody binding experiments on mice bearing BT474 xenograft

Purified scFv antibodies 799 and 785 for positive binding and 807 for negative control scFv were labeled with XenoLight CF680 fluorescent dye. One mg of scFv antibody was incubated with 0.1umol CF680-succinimidyl ester in 1 ml 0.1M $NaHCO_3$ solution (pH=8.3) and was stirred for 2 hours at room temperature in the dark. Free dye was removed by 30Kd cutoff Amicon Ultra-15 centrifugal filter (Millipore Corp, Billerica, MA). Degree of labeling (DOL) was determined by measurement of A280 and A680 and calculated based on the formula provided by manufactory protocol. The labeled scFv bound 1-2 dye molecules per antibody and did not lost its affinity to BT474 cells. For each mouse, 1 nmol fluorescence dye-labeled scFv antibody was intravenously injected into BT474 xenograft mice. Animals were scanned by Xenogen IVIS Lumina Imaging system at a series of time points after injection.

Figure 11 shows in vivo imaging results of scFv 785, 799, and 807 in mice bearing BT474 xenograft. These in vivo imaging results show that scFvs 799 and 785 have preferential accumulation in mouse kidney with no identifiable uptake in the tumor.

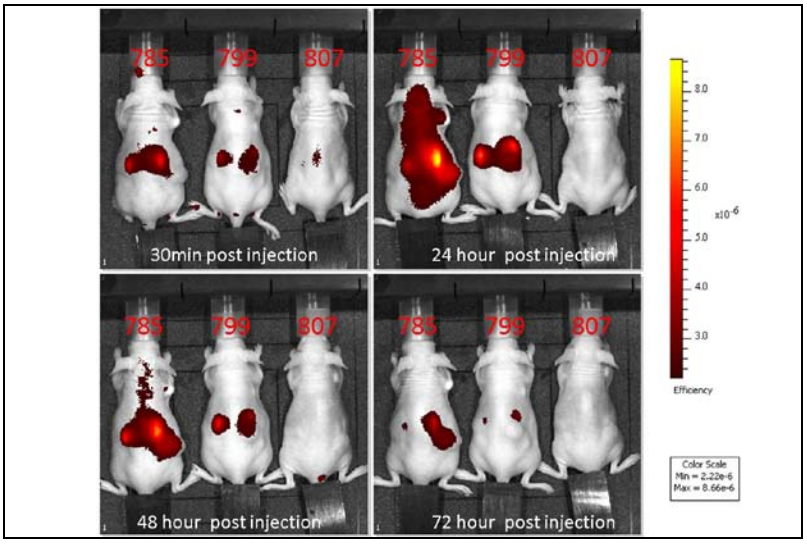

Figure 11: In vivo fluorescence images of nude mice bearing BT474 xenografts after i.v injection of scFvs.

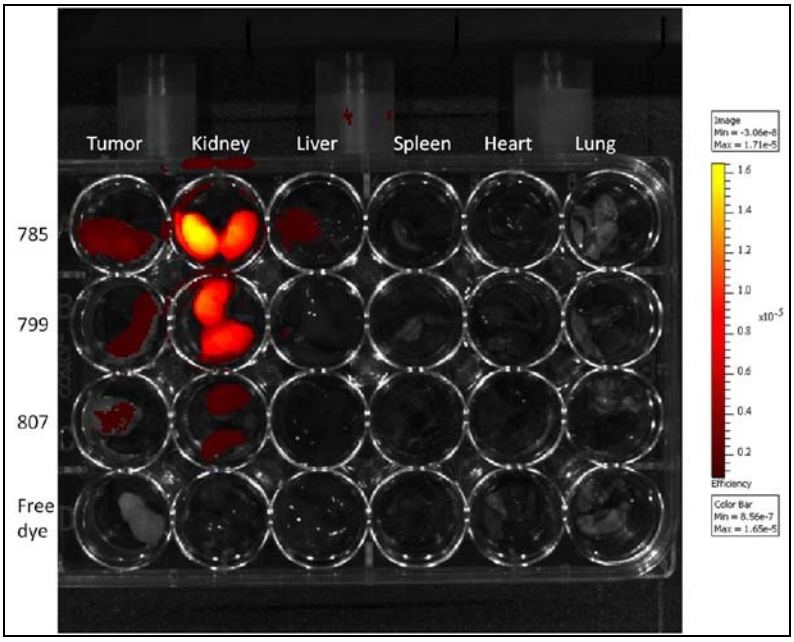

Figure 12: ex vivo fluorescence images of dissected organs of mice bearing BT474 xenograft tumor sacrificed 72 hours after i.v injection

72 hours after intravenous injection of scFvs and completion of all in vivo imaging the mice were sacrificed. The tumor and organs were harvested and then immediately imaged. Figure 12 shows images of organs and tumor harvested from the mice imaged in Figure 11. This harvested tissue confirms with in vivo images that there was preferential accumulation of scFvs 799 and 785 in the kidney compared to the BT474 xenograft.

It is likely that the smaller format of the scFv compared to full size antibody contributed to higher uptake in the kidney rather than the tumor. Options to resolve this problem include converting the 799 and 785 scFvs to IgG format. However this is beyond the scope of this grant.

2b-2. Using anti-ErbB2 and EpCAM monoclonal antibodies as modal antibodies for in vivo imaging experiment.

The goal of this proposal was to demonstrate increased overall binding in a solid tumor using antibodies to different tumor elements. The notion was that the target cells representing different tumor elements would include cancer cells and noncancer stromal cells. Strategies employed to this point did not yield the experimental conditions to evaluate increased overall tumor uptake using different antibodies. We therefore elected to use two antibodies that bind to different targets on BT474 cancer cells.

2b-2-1. Herceptin and anti-EpCAM antibodies are two strong binding antibodies to BT474 xenograft.

BT474 cancer cells overexpress both ErbB2 and epithelial cell adhesion molecule (EpCAM). Antibodies were selected that are known to bind each of these targets and are available.(Wang, Rayburn et al. 2006; Went, Vasei et al. 2006) The binding of Herceptin (monoclonal antibody binding to ErbB2, Genentech, Inc, CA) and anti-EpCAM antibody (R&D Systems, Inc) was evaluated on BT474 xenograft frozen sections. Figure 13 shows the staining results of Herceptin and anti-EpCAM antibody on BT474 xenograft. The results show strong binding to BT474 xenograft tissue by Herceptin and anti-EpCAM antibody (Figure 13, A and B). Isotype negative control showed no identifiable binding (Figure 13, C) These two antibodies were labeled with Xenogen fluorescence dye based on labeling protocol (See detail description in 2b-1). In order to observe the biodistribution of these two antibodies separately, Herceptin is labeled with CF680 while anti-Epcam antibody is labeled with CF770. The average DOL of these two antibodies is 3-4 dye molecules per antibody and the labeling did not interfere with antibody affinity to BT474 cells.

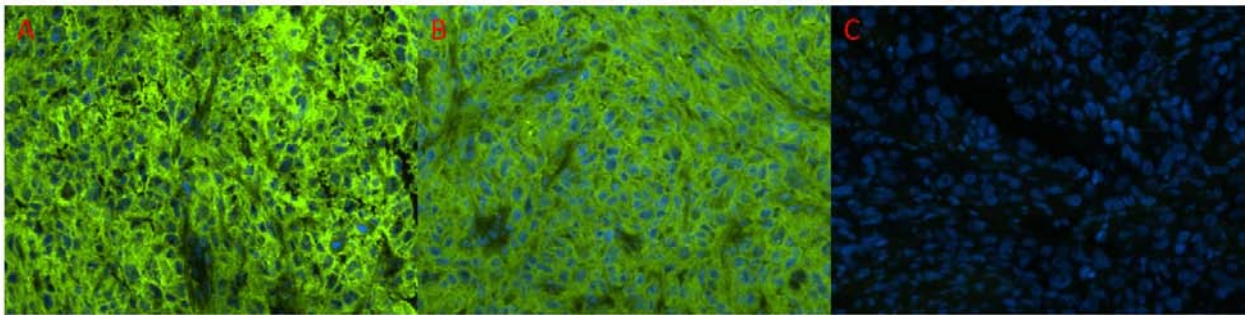

Figure 13: *Immunofluorescence (IF) analysis of Herceptin (A) and anti-EpCAM antibodies (B) on BT474 xenograft frozen slides. Isotype negative control antibody (C). Green is the antibody and blue is nuclear DAPI stain.*

2b-2-2. Evaluation of Xenogen IVIS Lumina imaging system to simultaneously image two antibodies labeled with different dyes.

The Xenogen IVIS Lumina imaging system has five filter sets which allow simultaneous or sequential imaging of different labeled reagents. We evaluated this system to image the chosen dyes in vitro to insure a good signal for each labeled antibody with minimal leaking of signal between dyes. Serial dilutions of labeled Herceptin-CF680 and EpCAM-CF770 were placed in 24-well plates for imaging with different filter sets. Figure 14 shows the same plate imaged with

two different filter combinations. The first column is Herceptin-CF680 solution with the highest to lowest concentration from the top row to bottom row. The last column contains anti-EpCAM-CF770 antibody solution also showing the concentration from highest to lowest, top to bottom. The two wells in the middle (row 2, columns 3 and 4) showing bright on both filter sets have both Herceptin-CF680 and EpCAM-CF770 in a 1:1 mixture. The left-hand image shows signal from Herceptin-680 and used the filter set Exc/Emi 675/cy5.5. Under this filter condition, only Herceptin-680, present in the first column and the two middle wells, has signals. The right-hand picture shows the imaging under filter sets (Exc/Emi 745/ICG). Under this filter condition, only anti-EpCAM -770 has a signal. This image shows EpCAM -770 in the far-right column and the middle two wells have signals. No signal leaking is observed under these filter sets, chosen for the subsequent in vivo imaging experiments.

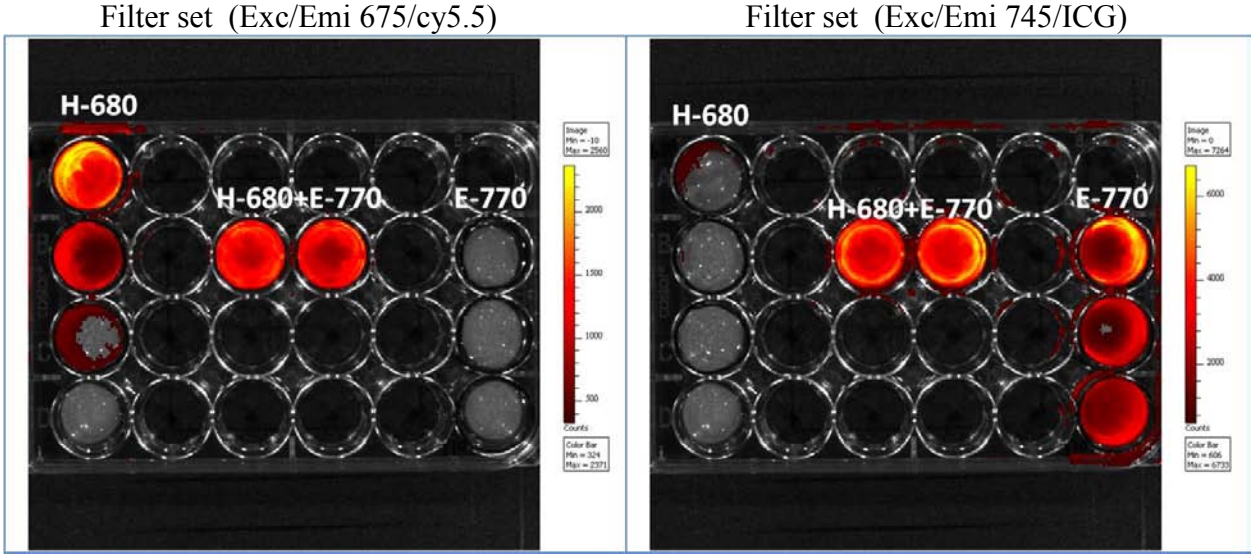

Figure 14: 24-well plates with Herceptin-680 in the first column and EpCAM -770 in the last column. The two middle wells (row 2, columns 3 and 4) have a 1:1 mixture of the two antibodies. The left picture shows the scan picture under filter sets (675, cy5.5), the right picture shows the scan picture under filter sets (745, ICG).

2b-2-3. In vivo imaging experiment on Herceptin and anti-EpCAM antibodies.
2b-2-3-1. in vivo imaging on NIR dye labeled Herceptin antibody

Mice bearing BT474 tumor were injected via the tail vein with 1 nmol Herceptin-680, 1 nmol negative antibody-680, and free dye with the same amount with antibody sample. Mice were anesthetized with isoflurane (Webster Veterinary, USA) and images were obtained at 0.5, 24, 48, and 96 hours after injection of each fluorescent antibody. The tumor areas were designated as regions of interest (ROI). The fluorescent efficiency of each ROI was obtained by IVIS in vivo imaging software.

In Figure 15, each panel of three mice shows different time points after injection of antibody. The upper left panel is time 0.5hrs, upper right is 24hrs, lower left is 48hrs and lower right is 96hrs. The first mouse in each panel was injected with Herceptin-CF680. The middle mouse was injected with negative control antibody680. The third mouse was injected with free dye 680. These series of images show preferential accumulation of Herceptin-CF680 in the BT474 xenograft compared to negative control antibody-CF680 and the free dye CF680.

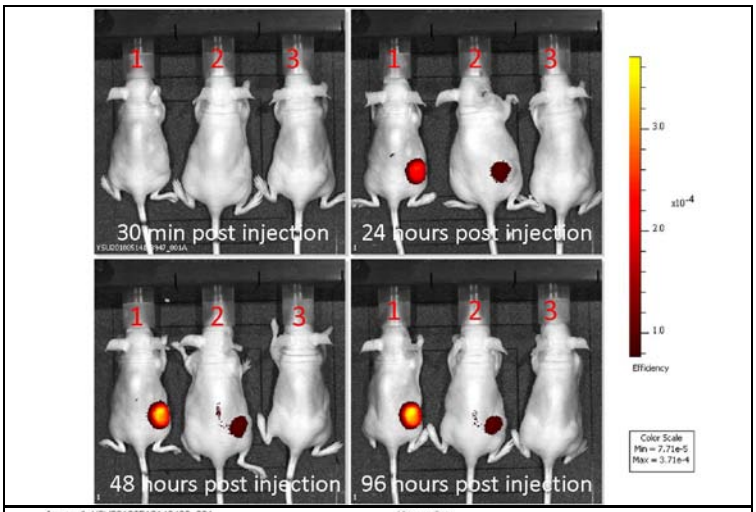

Figure 15: In vivo fluorescence imagines of nude mice bearing BT474 xenografts after i.v injection of Herceptin-CF680 (mouse no.1), negative control antibody 680 (mouse no.2), and free dye 680 (mouse no.3) at 0.5, 24, 48, and 96 hours post injection.

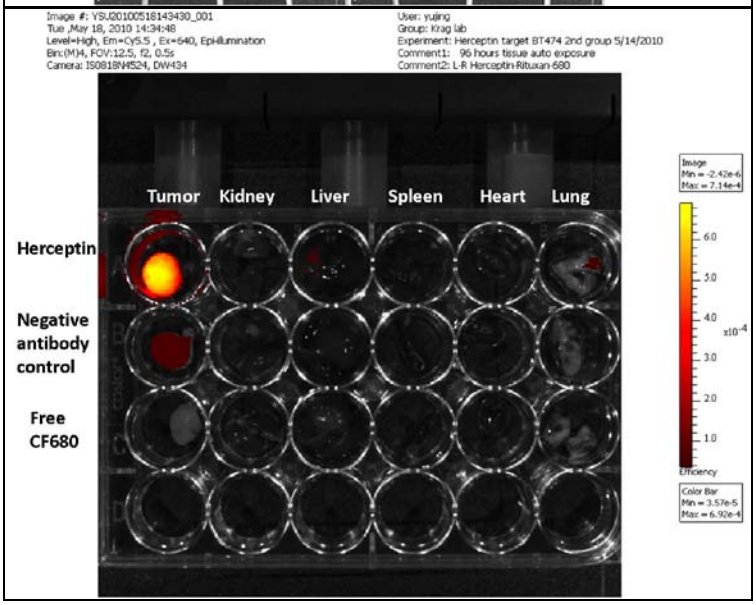

Figure 16: ex vivo fluorescence images of dissected organs of mice bearing BT474 xenograft tumor sacrificed 96 hours after i.v injection of Herceptin-CF680, negative control antibody 680, and free dye 680.

After the last in vivo images at 96 hours post injection, the mice were sacrificed and tumor and major organs were harvested for ex vivo imaging. Figure 16 shows the tumor and major organs for each mouse. The upper row is from the mouse injected with Herceptin-CF680. The second row is from the mouse injected with negative antibody control 680 and the third row is from the mouse injected with free dye 680. The first column is tumor and the next columns are kidney, liver, spleen, heart, and lung. These images show strong uptake of Herceptin-CF680 in the tumor and no uptake in the normal organs. Negative antibody control 680 and free dye 680 showed no uptake in the tumor or organs.

2b-2-3-2. In vivo imaging on NIR dye labeled anti-EpCAM antibody

Using the same methods described in 2b-2-3-1, three mice bearing BT474 xenografts were injected with either EpCAM-CF770, negative control antibody CF770, or free dye 770 and serially imaged to 96 hours. Filter sets were Exc/Emi 745/ICG.

In Figure 17, each panel of three mice shows different time points after injection of antibody. The upper left-hand panel is at 0.5 hours, the upper right-hand panel is at 24 hours, the lower left-hand panel is at 48 hours, and the lower right-hand panel is at 96 hours. The first mouse in each panel was injected with EpCAM-CF770. The middle mouse was injected with negative control antibody CF770. The third mouse was injected with free dye 770. These series of images show preferential accumulation of EpCAM-CF770 in the BT474 xenograft compared to negative control antibody and the free dye 770.

After the last in vivo images at 96 hours post injection, the mice were sacrificed and tumor and major organs were harvested for ex vivo imaging. Figure 18 shows the tumor and major organs from each mouse. The upper row is from the mouse injected with EpCAM-CF770. The second and third rows are from the mouse injected with negative control antibody CF770, and the fourth row is from the mouse injected with free dye 770. The first column is tumor and the next columns are kidney, liver, spleen, heart, and lung.

These images from Figures 17 and Figure 18 show preferential accumulation of EpCAM-CF770 in the tumor with some minor uptake in the kidney and no uptake in other normal organs. Negative antibody 770 and free dye 770 showed no uptake in the tumor or normal organs.

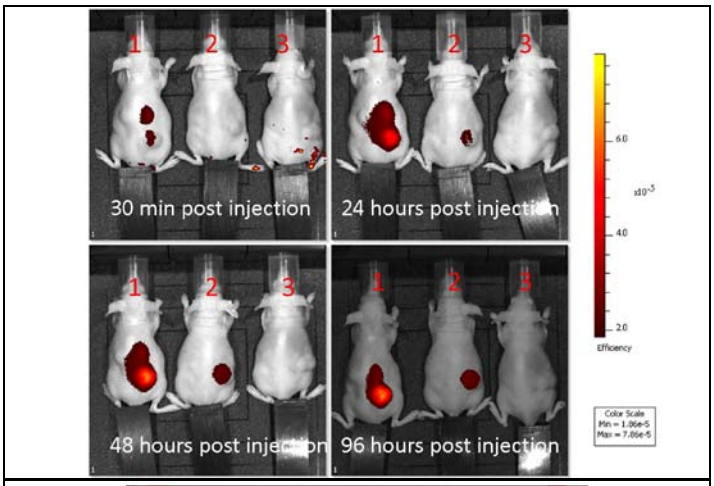

Figure 17: In vivo fluorescence images of nude mice bearing BT474 xenografts after i.v injection of Anti-Epcam-CF680 (mouse no. 1), negative control antibody 680 (mouse no.2), and free dye 680 (mouse no. 3) at 0.5, 24, 48, and 96 hours post injection.

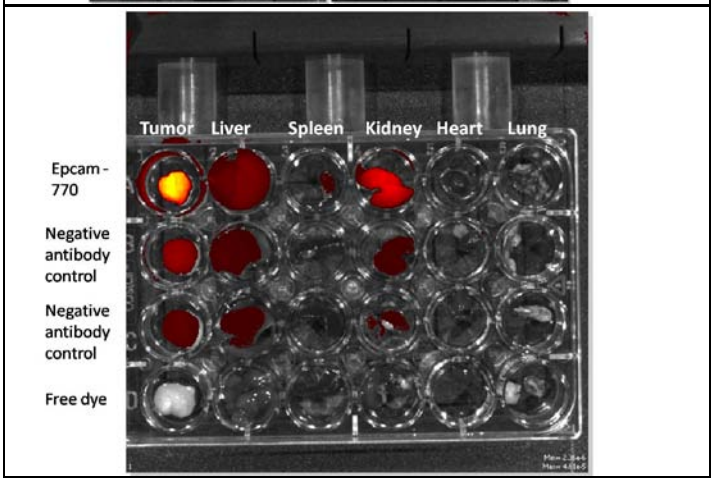

Figure 18: ex vivo fluorescence images of dissected organs of mice bearing BT474 xenograft tumor sacrificed at 96 hours after i.v injection of EpCAM-CF770, negative antibody control, and free dye 770

2b-2-3-3. In vivo imaging on simultaneous administration of Herceptin and anti-EpCAM antibody.

Herceptin-CF680 and EpCAM -770 antibodies were labeled with different xenograft CF dye and 1:1 cocktail were made for in vivo imaging.

Mice with BT474 xenografts were injected with either 1nmol Herceptin-CF680, 1nmol EpCAM-CF770, or a 1:1 mixture of Herceptin-CF680 and EpCAM-CF770 each at 1nmol. Three mice were used for each experiment, and this experiment was repeated three times for a total of 9 mice.

Figure 19 shows the 96-hour-post-injection in vivo images of one group of mice under two different filter sets. The left-hand panels of 3 mice are with the filter set of CF680 which only collects the signal of Herceptin. The right-hand panel is the same three mice using the filter set of CF770 which only collects the signal of anti-EpCAM antibody. The mouse on the left-hand side was injected with Herceptin. The mouse in the middle was injected with Herceptin and anti-EpCAM antibody and the mouse in the right-hand panel was injected with anti-EpCAM antibody. These images show that Herceptin and anti-EpCAM antibodies bound preferentially to the BT474 tumor in the condition of single antibody injection or when injected as a cocktail with a partner antibody.

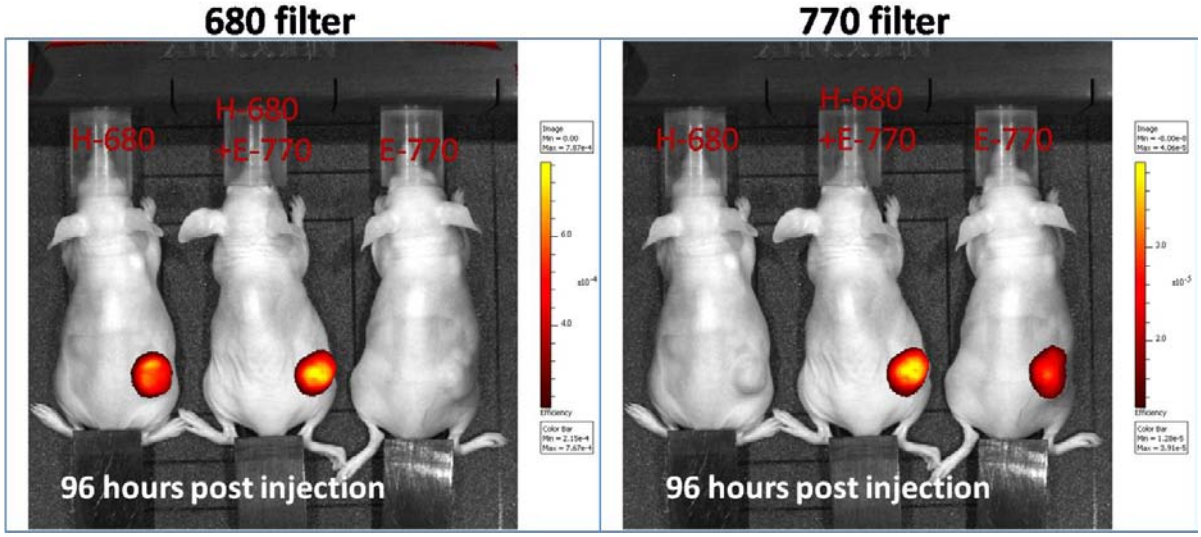

Figure 19: In vivo fluorescence images of nude mice bearing BT474 xenografts 96 hours after i.v injection of Herceptin-CF680 (mouse on left in each panel), mixture of Herceptin-CF680 and EpCAM-CF770 (middle mouse), and EpCAM-CF770 (mouse on right). The left-hand panel of three mice used filter set showing Herceptin and the right-hand panel of three mice used filter set showing signal from EpCAM-CF770.

The signal intensity over the tumor was measured serially over 144 hours for each experimental condition. Figure 20 illustrates the total relative fluorescence efficiency with the time after injection. Box A shows tumor uptake of Herceptin in mice given as the only antibody (blue line with diamonds) and as a cocktail with anti-EpCAM antibody (reddish line with squares). Herceptin antibodies quickly reach the peak level and keep that level up to 144 hours post injection. Box B shows tumor uptake of anti-EpCAM antibody in mice given as the only antibody (blue line with diamonds) or as a cocktail with Herceptin (reddish line with squares).

The tumor uptake of anti-EpCAM antibodies reach a peak at 48 hours (Fig 20-B) and gradually decrease until 144 hours.

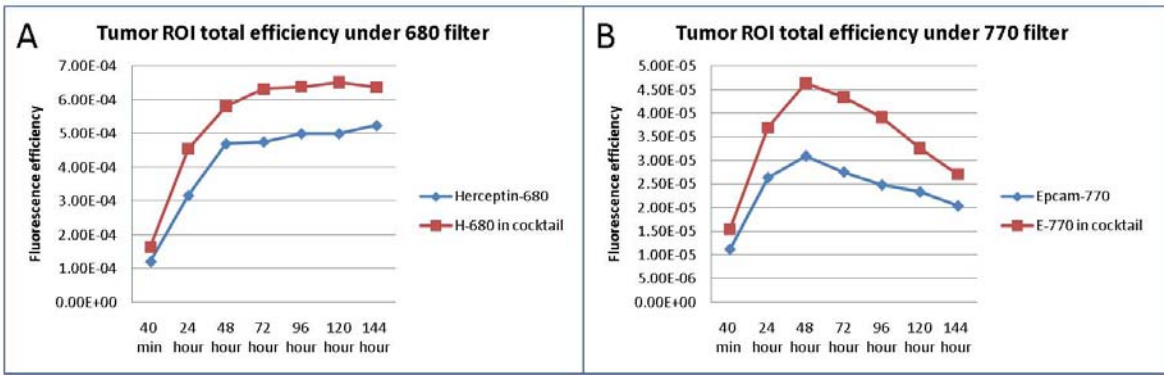

Figure 20: Total fluorescence efficiency in tumor ROI in mouse with BT474 xenograft i.v injected with Herceptin 680, anti-EpCAM-770, and cocktail.

These results show that accumulation of Herceptin-680 and EpCAM -770 is additive in that they do not interfere each other's binding affinity to tumor tissue in vivo.

Conclusion and Key Research Accomplishments

- BT474 xenograft model was successfully established in our lab. Tumor stroma enriched BT474 model was tested using BT474 cell lines and human breast fibroblast cell lines. Mixture of BT474 cells and human breast fibroblast cells did not yield a xenograft with sufficient fibroblast component.
- LCM panning of human tumor specimens was performed with selection on blood vessels. More than 200 monoclones were evaluated for binding. Although clones were identified with some blood vessel binding the affinity was too low for subsequent in vivo imaging studies.
- Three BT474 cell binding scFv clones 799, 785, and 794 were selected and single chain antibody of these clones were successfully expressed, purified, and prepared in large scale. These scFvs were evaluated in vivo but preferential binding to the tumor relative to normal tissue (especially kidney) was not sufficient.
- Antibodies that bind different targets on BT474 cells were selected and successfully labeled with infrared fluoresce dyes of different wavelengths. The labeling procedure was shown to not interfere with antibody affinity.
- The labeled antibodies (Herceptin and anti-EpCAM) were administred in vivo and successfully demonstrated to bind preferentially and additively in the tumor xenograft.

Reportable Outcomes

There have been no reportable outcomes yet.

References

Golchin, M. and R. Aitken (2008). "Isolation by phage display of recombinant antibodies able to block adherence of Escherichia coli mediated by the K99 colonisation factor." Vet Immunol Immunopathol 121(3-4): 321-31.

Shukla, G. S. and D. N. Krag (2005). "Phage display selection for cell-specific ligands: development of a screening procedure suitable for small tumor specimens." J Drug Target 13(1): 7-18.

Shukla, G. S. and D. N. Krag (2005). "A sensitive and rapid chemiluminescence ELISA for filamentous bacteriophages." J Immunoassay Immunochem 26(2): 89-95.

Wang, H., E. R. Rayburn, et al. (2006). "Immunomodulatory oligonucleotides as novel therapy for breast cancer: pharmacokinetics, in vitro and in vivo anticancer activity, and potentiation of antibody therapy." Mol Cancer Ther 5(8): 2106-14.

Went, P., M. Vasei, et al. (2006). "Frequent high-level expression of the immunotherapeutic target Ep-CAM in colon, stomach, prostate and lung cancers." Br J Cancer 94(1): 128-35.

Yashiro, M., K. Ikeda, et al. (2005). "Effect of organ-specific fibroblasts on proliferation and differentiation of breast cancer cells." Breast Cancer Res Treat 90(3): 307-13.